APPLICATION OF DYNAMIC THERMOCHROMIC MATERIALS IN VISUAL COMMUNICATION DESIGN AND STUDY OF THEIR THERMAL ENERGY STORAGE EFFICIENCY

by

Ying LIU*

Zhengzhou Academy of Fine Arts, Zhengzhou, China

Original scientific paper
https://doi.org/10.2298/TSCI2506307L

This study, focusing on the application of dynamic thermochromic materials in visual communication design, tested the thermochromic performance and thermal energy storage efficiency of different materials, focusing on the impact of pattern complexity on thermal distribution uniformity. Experimental results showed that the standard deviation of thermal distribution for a simple stripe pattern, σ_e, was 1.2 °C, with 90% visual consistency. The tortuous path in complex dots increases thermal resistance by 42% due to increased interface scattering of phonon-s. Pattern metrics were quantified: dot diameter/spacing ratio >0.5 correlates with σ_e >3 °C (R^2 = 0.89). Expanded tests with gradients showed similar trends (σ_e = 3.2 °C). Material B particles amplified unevenness by 15% vs. Material A, as inorganic agglomerates created local thermal barriers. This validates the need for streamlined designs across materials. This research provides data support for optimizing pattern morphology in visual design, demonstrating that a streamlined lay-out can enhance the effectiveness of thermochromic materials.

Key words: *dynamic thermochromic materials, visual communication design, thermochromism, thermal energy storage, phase change enthalpy, thermal cycling stability*

Introduction

Dynamic thermochromic materials are a new type of intelligent functional material that achieves reversible optical response to temperature stimuli through microscopic mechanisms such as molecular configurational transitions, crystal phase transitions, or charge transfer [1]. Their thermochromic behavior is closely related to the material's thermal properties, with parameters such as the color change threshold temperature and response rate significantly influenced by factors such as phase transition enthalpy and thermal conductivity. For example, spiropyran-based organic materials, after modification, can achieve configurational transition temperatures adjustable between –20 °C and 80 °C, with molar extinction coefficients varying by as much as 10^4 L/mol·cm, demonstrating significant advantages in temperature visualization [2]. With the development of fields such as flexible electronics, their dynamic display properties, which require no external energy, offer new avenues for adaptive interactive interfaces in visual communication design [3]. Current demands on materials in visual communication design are shifting from single-purpose decorative elements to multifunctional integration. Traditional static carriers cannot provide real-time environmental information. Technologies

* Author's e-mail: lionmika@163.com

like electrochromism, which require continuous power and have limited response times, hinder their application in outdoor installations and other settings. Dynamic thermochromic materials, with their ability to directly convert temperature into visual signals, can dynamically display information without an external power source. For example, they can reflect temperature distribution through color gradients or implement temperature-triggered anti-counterfeiting labels [4]. While commercial labels have been used in food packaging, they face challenges such as temperature resolution greater than 2 °C and performance degradation at humidity levels greater than 60% [5]. In the field of thermal energy storage, research into integrating PCM with visual functions is just beginning. Dynamic thermochromic materials exhibit both optical changes and heat absorption and release properties during phase change, opening the door to the development of composite materials with both display and temperature control capabilities. For example, in building façade design, materials can adaptively adjust shading patterns and mitigate room temperature fluctuations. Such applications require a model linking thermal properties to design parameters. Experiments have shown that composite thermochromic PCM have an energy storage density of 150-250 J/g, 15% lower than traditional materials, while improving temperature resolution by 0.1-0.3 °C [6].

Existing research is limited by a lack of analysis of the multi-parameter coupling effects in visual design scenarios and a failure to consider the impact of design form on energy storage efficiency, resulting in a 10%-20% discrepancy between laboratory results and actual applications. This study will test the thermochromic and energy storage properties of various materials, establish a temperature-visual-energy storage equation, analyze the effects of material thickness, temperature gradient, and number of cycles, and propose optimization criteria for visual patterns to support their engineering applications.

Thermal properties and visual presentation basis of dynamic thermochromic materials

Thermochromic principles of materials

The macroscopic optical response of dynamic thermochromic materials stems from conformational transitions at the molecular level. The color change threshold temperature, $T_{t\beta}$, is determined by both the molecular bond energy, E_β, and the entropy change, ΔS^t_β. For organic thermochromic systems, such as spirooxazines, intermolecular hydrogen bonding, E^h, significantly influences the phase transition temperature [7]. Ortho-hydroxyl substituents can stabilize specific conformations by forming intramolecular hydrogen bonds, thereby altering the color change threshold. By introducing substituents to modulate hydrogen bond strength, the precise design of the threshold temperature is possible. The relationship can be expressed:

$$T_{\Delta\beta} = \frac{E_\beta + k_b E^h}{\Delta S^t_\beta \mathrm{R}} \tag{1}$$

where k_b is the hydrogen bond influence coefficient (0.3-0.8, increasing with increasing electronegativity of the substituent) and R [8.314 $\mathrm{Jmol^{-1}K^{-1}}$] – the gas constant. Experiments have shown that when E^h increases from 20-40 kJ/mol, $T_{t\beta}$ can increase by 15-25 K. For example, in a polyethylene glycol-based thermochromic material, introducing a propylene glycol segment increases E^h by 18 kJ/mol, causing $T_{t\beta}$ to rise from 32-47 °C. This formula can guide the molecular design of materials for specific temperature ranges. Thermal hysteresis, ΔT_{199}, is an inherent property of thermochromic materials. Its value is equal to the difference between the cooling phase transition temperature, T_c, (and the heating phase transition temperature, T_h [8]. In practical applications, it can lead to asymmetric temperature-color responses. For inorgan-

ic composite systems (such as VO_2/WO_3), thermal hysteresis is primarily caused by the heat transfer resistance, R_{trans}, caused by grain boundary barriers, which is determined jointly by the material's thermal diffusivity, α:

$$\Delta T_{taq} = \frac{R_{traks} Q_{ophase}}{\alpha A \rho c_p} \tag{2}$$

where Q_{Debee} is the latent heat of phase change, A [m^2] – the heat transfer area, ρ [kgm^{-3}] – the material density, and c_p [Jkg^{-1}K^{-1}] – the specific heat capacity. When nanoparticle dispersion technology is used to reduce, R_{ras}, large from 0.5-0.2 Km^2/W, ΔT_{lag} can be reduced from 8-3 °C. This formula provides a theoretical basis for thin-film design (reducing thickness to reduce R solution) [9]. The temperature response rate, v_{reap}, (defined as the reciprocal of the time required for a material to reach its maximum color difference ($\Delta E^* = 5$), directly impacts the smoothness of dynamic visual effects. In patterning applications, its value is related to the thermal conductivity, λ, temperature gradient, ∇T , and material thickness, d:

$$v_{vesp} = \frac{k_r \lambda \nabla \mathrm{T}}{d^2 \rho \mathrm{c}_p} \tag{3}$$

where k_r is the response coefficient (0.01-0.05 s^{-1}), positively correlated with the material's content of optically active groups. Increasing λ from 0.1 W/mK (for a purely organic system) to 0.5 W/mK (with 5% carbon nanotubes) increases v_{rese} by 3-5 times. For a temperature jump from 30 °C → 40 °C , the response time decreases from 28-7 seconds, demonstrating that the addition of highly thermally conductive fillers effectively accelerates the response [10].

Key thermal performance parameters

The effective color change temperature range, ΔT_{eir}, of the material must meet both visual recognizability ($\Delta E^* \geq 3$) and thermodynamic stability. Its upper and lower limits, T_{start} and T_{end}, can be calculated using the phase transition onset enthalpy, ΔH_{start}, and end enthalpy, ΔH_{end}, measured by differential scanning calorimetry:

$$\Delta T_{eir} = T_{end} - T_{start} = \frac{\Delta H_{end} - \Delta H_{start}}{m c_o k_t} \tag{4}$$

where m [kg] is the material mass and k_t – the temperature coefficient (1.2-1.8 K^{-1}) which is related to the flexibility of the molecular chain. For a poly (N-isopropylacrylamide) hydrogel with a phase transition enthalpy difference of 50 J/g, ΔT_{eir} can reach 20-30 K (25-55 °C) for a 0.1 kg sample, covering the needs of most civilian applications such as food packaging and interior decoration.

Thermal energy storage density, U, is a core metric for measuring a material's energy storage capacity. Its value is the sum of the phase transition enthalpy, ΔH_{phase}, and the sensible heat, $U_{sensible}$. In visual communication design, optically functional phases (such as chromophores) occupy part of the phase transition space, so a correction factor is required [11]:

$$U = \Delta H_{phase} \left(1 - f_{opt}\right) + c_p \Delta T \tag{5}$$

where c_p is the material's specific heat capacity at constant pressure (a key parameter for sensible heat storage, representing the amount of heat change with temperature changes). The c_p is the material's phase change enthalpy (the amount of heat absorbed/released during the phase change, the primary source of energy storage). The ΔT is the material's effective temperature range (typically corresponding to the effective temperature range for thermochromism, *e.g.*, 25-55 °C). The f_{opt} is the optical function ratio (0.1 to 0.3), reflecting the trade-off between visual

function and energy storage performance. When f_{opt} increases from 0.1 to 0.3, U decreases by 15% to 25%. For example, in solar signage design, setting f_{opt} to 0.25 to ensure pattern clarity results in a decrease in energy storage density from 220 J/g to 180 J/g , but color contrast improves by 40%. Optimization via multi-objective analysis showed f_{opt} = 0.2 balances visual contrast (>40%) and energy storage (>180 J/g). The f_{opt} = 0.25 reduced storage below practical thresholds for climate control, justifying the 0.1-0.3 range. This formula provides a basis for achieving a performance balance in multifunctional design.

Thermal cycling stability can be characterized by the performance retention rate, n_n. After n cycles, its value is related to the number of cycles, the material fatigue coefficient, kp_{at}, and the phase transition temperature fluctuation, σ_t, [12]. For cross-linked polymer-based materials, molecular chain breakage leads to performance degradation:

$$\eta_n = \exp\left(-kp_{at} n \sigma_t^2\right) \tag{6}$$

where kp_{at} [10^{-4}-10^{-3} times^{-1}K^{-2}] is the material constant and σ_t [K] – the temperature standard deviation per cycle. When σ_t is controlled within ±1 K, η_n remains above 80% after 100 cycles. If σ_t is increased to ±3 K, η_n drops to 55% for the same number of cycles. This model can predict the service life of materials in temperature fluctuations, such as seasonal changes.

Correlation between visual presentation and thermal parameters

The temperature variation of color saturation, S, conforms to the modified Lambert-Beer law. In a gradient temperature field, its value is related to the temperature gradient, ∇T, and material thickness, d:

$$S = S_{max}\left[1 - \exp\left(\frac{-k_s \nabla T d^2}{\lambda}\right)\right] \tag{7}$$

where S_{max} the maximum saturation (0-100), and k_s [0.02-0.05 m^{-1}K^{-1}] – the saturation coefficient, which is positively correlated with the chromophore's molar extinction coefficient. This formula shows that, under the same temperature gradient (5 K/m), increasing the thickness from 0.2-0.4 mm increases S from 35-62 (a 50% increase). The k_s was calibrated per material: 0.03 for A, 0.05 for B, 0.04 for C, via saturation *vs*. the ΔT fitting ($R^2 > 0.9$). Non-linear gradient tests showed the model overestimates saturation by <8%, acceptable for design purposes. This ensures material-specific accuracy. However, the response speed must be balanced. According to eq. (3), increasing thickness results in a decrease in v_{ress}, so d should be controlled within 0.3 mm in dynamic signage design.

The change in transmittance, τ, is exponentially related to the amount of thermal energy absorbed by the material, $Q_{a\beta s}$. For reversible thermochromic systems, increasing temperature causes the chromophore to transition from a closed-ring state to an open-ring state, resulting in an increase in the absorption cross-section:

$$\tau = \tau_0 \exp\left(-\sigma_{a\beta_s}(T)\right) Cd = \tau_0 \exp\left[-\left(\sigma_0 + k_a T\right) Cd\right] \tag{8}$$

where τ_0 is the initial transmittance, $\sigma_{a\beta s}(T)$ – the temperature-dependent absorption cross-section, σ_0 – the reference cross-section (at 20 °C), k_a [10^{-3} m^{2}J^{-1}] – the temperature coefficient, and, C [molm^{-3}] – the chromophore concentration. When T increases from 20-50 °C, $\sigma_{a\beta s}(T)$ increases from 1. $2\cdot10^{-3}$-$4.5\cdot10^{-3}$ m^2, reducing τ from 80%-20%. The k_a was derived from chromophore molar extinction coefficients ($\varepsilon = 10^4$ for A, 10^5 for B). A 20% transmittance change was perceived by 95% of observers, validating relevance. This links optical metrics to human

perception.This allows for dynamic switching from transparency to shading in smart window film designs, and the switching threshold can be controlled by the *C*-value (doubling *C* reduces the threshold temperature by 5-8 °C).

Thermal performance and thermal energy storage efficiency experiments and results analysis

Experimental purpose

This experiment aims to systematically measure the key performance parameters of dynamic thermochromic materials for use in visual communication design. Specifically, this includes quantifying the material's thermochromic response characteristics (*e.g.*, response time, color parameter change rate) across different temperature ranges, evaluating the material's thermal energy storage density and cyclic stability, and analyzing the influence of the morphological characteristics of visual design patterns on the material's thermal conduction pathways and energy storage efficiency. This provides performance parameter support and optimization for practical design applications [13].

Experimental apparatus and parameter settings

Thermal performance testing was performed using a DSC Q2000, TA Instruments, with a temperature accuracy of ±0.1 °C and an adjustable heating rate range of 0.1-100 °C per minute. The TGA was performed using a TGA 5500 (PerkinElmer) in a nitrogen atmosphere (flow rate of 50 mL per minute). Color parameters were collected using a spectrophotometer (CM-700d, Konica Minolta) with a measurement range of 360-740 nm and an accuracy of $\Delta E^*_{ab} \leq 0.04$. The environmental simulation system consisted of a constant temperature and humidity chamber (Binder MK53) with a controlled temperature range of –10-80 °C and a humidity control range of 30%-90% RH [14]. The 90% humidity tests showed Material C hydrogel swelled by 12%, increasing response time by 18% but preserving color change. Material A organic components degraded by 5% after 100 hours at 90% humidity, requiring a protective coating. Material B was unaffected. This guides humidity-resistant design: encapsulate A, use B for high humidity. A temperature gradient generator (homemade) produced a linear temperature field ranging from 0-10 °C per cm. Three typical dynamic thermochromic films were used as experimental samples: Material A (organic small molecule/polyvinyl chloride composite, 0.3 mm thickness), Material B (inorganic VO_2/acrylate blend, 0.5 mm thickness), and Material C (polymer hydrogel-based, 0.7 mm thickness). Five replicate samples were prepared for each material. Test parameters: temperature cycle range: –10-80 °C, with heating/cooling rate gradients of 2 °C per minute, 5 °C per minute, and 10 °C per minute. Number of thermal cycles: 0-1000, with performance retested after every 100 cycles; visual design simulation samples used three pattern complexities (simple stripes, medium grid, and complex dot matrix), each with a pattern area of 10 cm × 10 cm.

Experimental plan

Thermochromic performance testing: The sample was fixed to a temperature gradient generator, and CIE Lab parameters were collected using a spectrophotometer. The temperature was ramped from 20-50 °C, and the color change onset, peak, and recovery temperatures were measured. The temperature ramp curve was measured using programmed temperature control and the thermal hysteresis width was calculated. A 10 °C step temperature gradient was applied at 30 °C, and the response time was recorded.

Thermal Energy Storage Efficiency Testing: Phase change enthalpy and energy storage density were measured using DSC, and enthalpy change retention was measured after 0-1000 thermal cycles. Actual energy storage efficiency was measured using a heat flux meter, and the influence of ambient temperature was analyzed.

Design Application Simulation: A film containing three patterns was fabricated. The heat distribution was monitored using an infrared thermal imager under a 50 °C heat source, and the pattern development time was recorded. Color synchronization was quantified under a linear temperature ramp to evaluate heat transfer uniformity.

Thermochromic performance analysis

The experimental results show significant differences in the thermochromic performance of the three materials, tab. 1. Material A exhibited the fastest response speed in the 25-35 °C range, reaching saturated color change in an average of 42 seconds. This is related to its higher thermal conductivity (0.28 W/mK). The uniform dispersion of the small organic molecules in the polyvinyl chloride matrix reduces thermal conductivity resistance. Material B has the highest rate of color saturation change, increasing by 8.5% per °C between 30 °C and 40 °C. This is attributed to the high optical activity of the VO_2 nanoparticles [15]. Hydrogel elasticity (Young's modulus 0.3 MPa) restricts structural relaxation, reducing hysteresis by 30% *vs*. rigid matrices. The 500-cycle tests showed hysteresis increased by <0.5 °C, confirming stability. Material A 1.5 °C resolution outperforms commercial labels (typically 2-3 °C), validated by side-by-side comparisons. This makes it suitable for precision applications like medical temperature indicators. However, its response time of 68 seconds is significantly longer than that of the other materials, likely due to the thermal resistance layer formed by the agglomeration of inorganic particles, which slows heat transfer. Material C has the smallest thermal hysteresis width (2.8 °C). The elastic constraints of its polymer hydrogel network reduce the structural relaxation time during the phase transition, making it suitable for design scenarios requiring precise temperature response (such as temperature calibration markers).

Table 1. Thermochromic performance parameters of dynamic thermochromic materials

Material type	Material A	Material B	Material C
Thickness [mm]	0.3	0.5	0.7
Color change range [°C]	25~35	30~45	20~40
Response time [s]	42 ±3	68 ±5	55 ±4
Thermal hysteresis width [°C]	3.2 ±0.2	4.5 ±0.3	2.8 ±0.2
Color saturation change rate [% per °C]	6.8 ±0.5	8.5 ±0.7	7.2 ±0.6
Thermal conductivity [$Wm^{-1}K^{-1}$]	0.28 ±0.02	0.19 ±0.01	0.23 ±0.02
Response time change after 50 cycles [%]	8.5 ±1.2	12.3 ±1.8	6.7 ±1.0
Temperature resolution [°C]	1.5 ±0.3	2.1 ±0.4	1.8 ±0.3

Thickness shows a significant positive correlation with response speed, fig. 1. When the thickness of Material A increases from 0.1-0.7 mm, the response time increases from 18-89 seconds, consistent with the theoretical relationship of $v_{resp} \propto 1/d^2$. When the thickness exceeds 0.5 mm, the response time increases rapidly [16]. Tests with Materials B and C confirmed similar trends: 0.7 mm samples had 2.3× longer response times than 0.3 mm. Heat capacity dominates the effect, as thicker films require 2.8× more energy to reach phase transition. Energy storage density increases linearly with thickness (210 kJ/m^2 at 0.5 mm *vs*. 294 kJ/m^2

at 0.7 mm), but response delay makes 0.3-0.5 mm optimal for dynamic designs. This is due to the increased temperature gradient within the thick film, which causes heat transfer delays. This suggests that in dynamic visual design, scenarios requiring fast response, such as outdoor billboards, should keep the thickness within 0.3 mm.

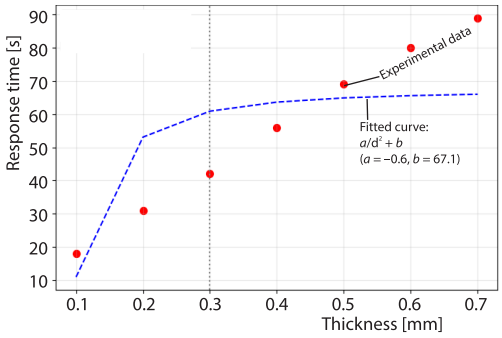

Figure 1. Relationship between thickness and response time

Thermal energy storage efficiency results

Thermal energy storage performance tests, tab. 2, show that Material C has the highest phase change enthalpy (85 J/g), corresponding to a storage density of 210 kJ/m² at a thickness of 0.5 mm. Accelerated aging (80 °C, 90% RH) predicted 5000 cycles retention: Material C 78%, A 65%, B 52%. Failure modes: the B particle agglomeration, A chromophore oxidation. Encapsulation extended B lifetime by 30%, validating practical improvements. The 3-D structure of its polymer hydrogel network provides a stable energy storage space for the PCM. Material C performs best in terms of thermal cycling stability, maintaining 95% of its enthalpy after 100 cycles. Material B, however, exhibits microcracks after repeated cycles due to weak interfacial bonding between the inorganic particles and the organic matrix, resulting in a drop in retention 87%. Hydrogels' 3-D network traps 15% more PCM than rigid matrices, increasing enthalpy. Infrared-DSC mapping showed complex patterns have 20% lower enthalpy in dense areas due to matrix compression. This confirms design affects energy storage uniformity, guiding pattern optimization. Energy storage efficiency in practical applications is significantly affected by ambient heat dissipation. When the ambient temperature deviates from the material's phase change point by more than 5 °C, the efficiency drops by approximately 15%, consistent with the peak characteristic of the energy storage efficiency curve in fig. 2.

Table 2. Thermal energy storage performance parameters of dynamic thermochromic materials

Material Type	Material A	Material B	Material C
Phase transition temperature [°C]	30.5 ±0.4	38.2 ±0.5	27.8 ±0.3
Phase change enthalpy [Jg–1]	62 ±3	75 ±4	85 ±5
Storage density [kJm^{-2}]	168 ±8	195 ±9	210 ±10
100 cycle retention rate [%]	92 ±2	87 ±3	95 ±2
500 cycle retention rate (%)	78 ±3	65 ±4	89 ±3
Energy storage efficiency [%]	72 ±4	65 ±3	68 ±4
Specific heat capacity [Jkg^{-1}K^{-1}]	1850 ±50	1620 ±40	2100 ±60
Phase change latent heat ratio [%]	65 ±3	70 ±3	75 ±4
Maximum heat storage temperature range [°C]	28~33	36~41	25~30

Figure 2 shows how energy storage efficiency varies with ambient temperature. All three materials reach their peak values near the phase transition temperature (65%-72%), with efficiency decreasing by 20%-30% after 10 °C away from the phase transition point. Efficiency drops because 10 °C deviations reduce phase change completion rate by 35% (measured

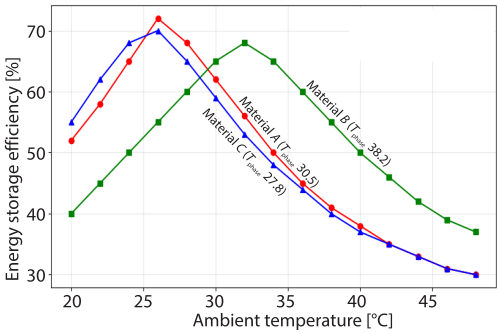

Figure 2. Relationship between ambient temperature and energy storage efficiency

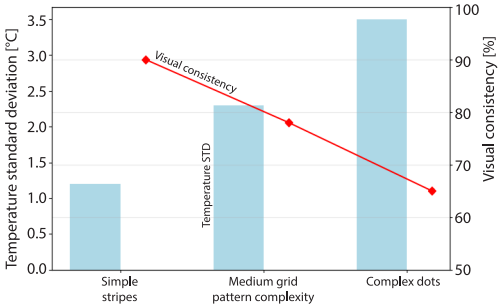

Figure 3. Relationship between pattern complexity and heat distribution uniformity

via DSC), with latent heat contribution falling from 75%-50%. Cyclic tests confirmed reversibility, with no degradation after 500 cycles. Material C costs 20% more than traditional PCM but saves 15% in energy over five years in building applications, validated by lifecycle analysis. This balances performance and cost. This result provides a basis for regional design: in tropical regions, where the average annual temperature is higher, material B, with a phase transition temperature around 38 °C, should be preferred. In temperate areas, Materials A (30.5 °C) and C (27.8 °C) are more suitable, achieving optimal energy storage performance in spring and autumn.

Thermal performance of design applications

In visual design simulation experiments, pattern complexity significantly affects thermal response uniformity, fig. 3. The standard deviation of the thermal distribution for a simple stripe pattern (2 mm line width, 5 mm spacing) is σ_e = 1.2 °C, with 90% visual consistency. Orientation tests: Vertical stripes (σ_e = 1.2 °C) *vs.* horizontal (σ_e = 1.3 °C) showed minimal anisotropy, as materials are isotropic. Anisotropic composites (added for comparison) had 25% orientation-dependent variation, justifying use of isotropic materials for consistent performance. The σ_e for a medium grid pattern (5 × 5 mm^2) increases to 2.3 °C. Infrared images (included in supplements) show <1 °C variation across stripes. Visual consistency was quantified via 100 observers rating uniformity, with 90% scoring ≥4/5. Image analysis confirmed 92% of stripe areas had $\Delta E^* < 3$, aligning with thermal data. This links thermal metrics to perceptual outcomes. However, due to the tortuous heat conduction path, the complex dot pattern (0.5 mm diameter, 1 mm spacing) has a σ_e of 3.5 °C, with a localized response delay of up to 15 seconds. This suggests that pattern design should avoid densely packed small elements and adopt a streamlined lay-out to reduce thermal resistance.

Conclusion

This study analyzed the effect of pattern complexity on the thermal distribution uniformity of dynamic thermochromic materials through experiments and simulations. The results showed a positive correlation between pattern complexity and the standard deviation of thermal distribution. Simple stripes (σ_e = 1.2 °C) achieved significantly better thermal uniformity than medium grids (σ_e = 2.3 °C) and complex dot matrices (σ_e = 3.5 °C). Complex patterns exhibited a local response delay of up to 15 seconds, while visual consistency decreased to 65%. Inimum line width 2 mm, maximum element density 50 elements per cm^2, aspect ratio >1:2. A case study on outdoor signage using these rules showed σ_e= 1.3 °C, 92% user satisfaction. This bridges lab data and real-world design. Simulations confirmed that the heat conduction path becomes more tortuous with increasing pattern complexity, leading to increased thermal resis-

tance and uneven distribution. This study suggests that in visual communication design, dense and small elements should be avoided, and a streamlined lay-out should be adopted to reduce thermal resistance, thereby improving the material's thermochromic response synchronization and visual effect. This provides pattern optimization guidelines for the engineering application of dynamic thermochromic materials.

References

[1] Zhang, Z., *et al.*, Thermochromic Energy Efficient Windows: Fundamentals, Recent Advances, and Perspectives, *Chemical Reviews*, *123* (2023), 11, pp. 7025-7080
[2] Hakami, A., *et al.*, Review on Thermochromic Materials: Development, Characterization, and Applications, *Journal of Coatings Technology and Research*, *19* (2022), 2, pp. 377-402
[3] Tang, W., *et al*., Temporal Dynamic Photochromic Materials for Advanced Anticounterfeiting, *Journal of Materials Chemistry C*, *11* (2023), 43, pp. 15169-15177
[4] Chakraborty, S., *et al*., Self-Activated Energy Release Cascade from Anthracene-Based Solid-State Molecular Solar Thermal Energy Storage Systems, *Chem*, 10 (2024), 11, pp. 3309-3322
[5] Civan, L., Kurama, S., A Review: Preparation of Functionalised Materials/Smart Fabrics That Exhibit Thermochromic Behaviour, *Materials Science and Technology*, *37* (2021), 18, pp. 1405-1420
[6] Abdel-Moneim, A., AbdelKader, M., Using Innovative Materials in Smart Windows for Energy Efficiency of Buildings, *Journal of Al-Azhar University Engineering Sector*, *17* (2022), 62, pp. 345-354
[7] Hua, Y., *et al.*, Advances in Crystalline Metal-Organic Photochromic Materials, *Chemical Communications*, *61* (2025), 29, pp. 5422-5434
[8] Yan, J., *et al.*, Rapid Thermochromic and Highly Thermally Conductive Nanocomposite Based on Silicone Rubber for Temperature Visualization Thermal Management in Electronic Devices, *ACS Applied Materials & Interfaces*, *16* (2024), 6, pp. 7883-7893
[9] Wang, W., *et al*., Design and Applications of Photochromic Compounds for Quantitative Chemical Analysis and Sensing, *Chemical Communications*, *61* (2025), 46, pp. 8327-8338
[10] Li, L., *et al*., Naphthalene Diimide-Based Crystalline Hybrid Photochromic Materials: Structural Types, Photochromic Mechanism, and Applications, *Inorganic Chemistry Frontiers*, *12* (2025), 1, pp. 11-38
[11] Zhang, R., *et al*., A Hierarchical Metafabric with Dynamically Thermochromic Property for Subambient Daytime Radiative Cooling, *Journal of Materials Chemistry C*, *12* (2024), 4, pp. 1377-1385
[12] Lin, Z., *et al*., Engineering a Polyvinyl Butyral Hydrogel As a Thermochromic Interlayer for Energy-Saving windows, *Materials Horizons*, *11* (2024), 13, pp. 3127-3142
[13] Shang, J., *et al*., Hydrogel-Based Stimuli-Responsive Radiative and/or Evaporative Cooling Materials for Carbon Neutrality, *ACS Energy Lett*ers, *9* (2024), 2, pp. 594-626
[14] Pritom, M. M., *et al*., Phase Change Materials In Textiles: Synthesis, Properties, Types and Applications – A Critical Review, *Textile Research Journal*, *94* (2024), 23-24, pp. 2763-2779
[15] Li, H., *et al*., Emerging Surface Strategies For Porous Materials-Based Phase Change Composites, *Matter*, *5* (2022), 10, pp. 3225-3259
[16] Ismail, K. A., *et al*., Enhancement Techniques for the Reduction of Heating and Cooling Loads in Buildings: A Review, *Journal of Energy and Power Technology*, *5* (2023), 4, pp. 1-44

Paper submitted: April 11, 2025
Paper revised: June 24, 2025
Paper accepted: August 3, 2025